

UC Berkeley

UC Berkeley Previously Published Works

Title

Thermal conductivity as a metric for the crystalline quality of SrTiO₃ epitaxial layers

Permalink

<https://escholarship.org/uc/item/07m656b0>

Journal

Applied Physics Letters, 98(22)

ISSN

0003-6951

Authors

Oh, Dong-Wook
Ravichandran, Jayakanth
Liang, Chen-Wei
[et al.](#)

Publication Date

2011-05-30

DOI

10.1063/1.3579993

Peer reviewed

Thermal conductivity as a metric for the crystalline quality of SrTiO₃ epitaxial layers

Dong-Wook Oh,^{1,a)} Jayakanth Ravichandran,² Chen-Wei Liang,³ Wolter Siemons,⁴ Bharat Jalan,⁵ Charles M. Brooks,⁶ Mark Huijben,⁷ Darrell G. Schlom,⁶ Susanne Stemmer,⁵ Lane W. Martin,³ Arun Majumdar,⁸ Ramamoorthy Ramesh,⁹ and David G. Cahill³

¹Energy Plant Research Division, Korea Institute of Machinery and Materials, Daejeon 305-343, Republic of Korea

²Applied Science and Technology Graduate Group, University of California, Berkeley, California 94720, USA

³Department of Materials Science and Engineering, and Materials Research Laboratory, University of Illinois, Urbana, Illinois 61801, USA

⁴Department of Physics, University of California, Berkeley, California 94720, USA

⁵Department of Materials, University of California, Santa Barbara, California 93106, USA

⁶Department of Materials Science and Engineering, Cornell University, Ithaca, New York 14853, USA

⁷Faculty of Science and Technology, University of Twente, Faculty of Science and Technology, 7500 AE Enschede, The Netherlands

⁸Department of Energy, ARPA-E, Washington DC 20585, USA

⁹Department of Materials Science and Engineering, University of California, Berkeley, California 94720, USA

(Received 23 November 2010; accepted 22 March 2011; published online 31 May 2011)

Measurements of thermal conductivity Λ by time-domain thermoreflectance in the temperature range $100 < T < 300$ K are used to characterize the crystalline quality of epitaxial layers of a prototypical oxide, SrTiO₃. Twenty samples from five institutions using two growth techniques, molecular beam epitaxy and pulsed laser deposition (PLD), were analyzed. Optimized growth conditions produce layers with Λ comparable to bulk single crystals. Many PLD layers, particularly those that use ceramics as the target material, show surprisingly low Λ . For homoepitaxial layers, the decrease in Λ created by point defects correlates well with the expansion of the lattice parameter in the direction normal to the surface. © 2011 American Institute of Physics.

[doi:10.1063/1.3579993]

In recent years, epitaxial growth of complex oxides with the perovskite crystal structure has figured prominently in studies of the physics of correlated electrons¹ and in the search for electronic materials for information technology and sensing.^{2,3} Traditionally, the main tools that are used to characterize the layers quality are x-ray diffraction (XRD) (Ref. 4) and transmission electron microscopy (TEM) (Refs. 5 and 6) and, in more limited cases, *in situ* reflection high-energy electron diffraction (RHEED).⁷ In the case of homoepitaxial growth, strain produced by point defects can be revealed by XRD. In the case of heteroepitaxy, however, lattice mismatch between substrate and film often obscures strain produced by defects. TEM is a powerful method for characterizing *extended* defects—e.g., dislocations and various types of planar defects—but point defect densities are not always accurately reflected in TEM images.⁸ Recently a number of new approaches such as diffuse x-ray scattering and optical fluorescence spectroscopies have been put forth to study and quantify crystal quality but these approaches are not applicable in general.⁹

Transport properties, on the other hand, often provide a sensitive probe of crystal quality. For epitaxial semiconductors, the Hall mobility is a common metric. Hall mobility is also a powerful tool for oxide semiconductors,¹⁰ the applicability is constrained because mobilities are sometimes intrin-

sically small and not all oxides are electrically conducting. Furthermore, stray electrical conductivity in substrates can confound electrical transport measurements on films.¹¹

Here, we describe the use of thermal conductivity as a tool for evaluating the quality of epitaxial layers of a prototypical perovskite oxide, SrTiO₃ (STO). The foundations of our approach have a long history: thermal conductivity has frequently been used in the past to evaluate the perfection of bulk nonmetallic crystals.¹² Near room temperature, the segments of the phonon spectrum that dominate heat transport have wavelengths of ~ 1 nm and, therefore, the lifetimes of heat-carrying phonons are highly sensitive to deviations from the periodicity of the crystal lattice that are produced by point defects and defect clusters.¹³

We measure Λ of STO films by time domain thermoreflectance (TDTR).^{14–16} STO films are prepared at five different institutions. Molecular beam epitaxy (MBE) samples were grown at the U. California Santa Barbara (MBE-1) and at Cornell U. (MBE-2). Pulsed laser deposition (PLD) was used to prepare samples at the U. California Berkeley, UCB (PLD-1), U. Twente (PLD-2) and U. Illinois, UIUC (PLD-3). A full description of the samples is listed in Table I of the supplementary information, see Ref. 17. The MBE-1 samples were grown by a “hybrid” MBE technique^{10,18} where a metal-organic precursor, titanium tetra isopropoxide (TTIP) is used as the Ti source; the oxygen beam equivalent pressure was 5×10^{-6} Torr; and the TTIP/Sr ratio was ≈ 42 MBE-1 films are grown on either single-crystalline (001)

^{a)}Electronic mail: dwoh@kimm.re.kr.

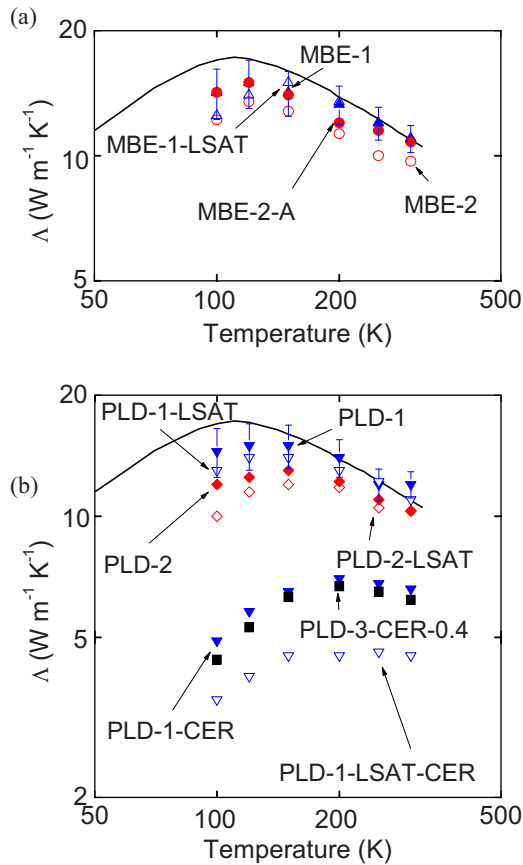


FIG. 1. (Color online) Thermal conductivity STO epitaxial layers. The solid line is data for bulk STO from Ref. 19. (a) Thermal conductivity of MBE grown films. (b) The notation “-CER” indicates that the samples were grown using ceramic STO as the laser target. Thermal conductivity of PLD grown films. Representative error bars are shown for (a) MBE-1 and (b) PLD-1 samples. Uncertainties in the other data points are comparable to these representative error bars at corresponding temperatures.

STO (MBE-1) or $(\text{LaAlO}_3)_{0.3}(\text{Sr}_2\text{AlTaO}_6)_{0.7}$ (MBE-1-LSAT) substrates. MBE-2 samples were grown by conventional MBE methods on STO substrates with the addition of $\approx 10\%$ ozone; the oxygen beam equivalent pressure was 5×10^{-7} Torr.²⁰ Two films were prepared: one sample was measured as-received (MBE-2), and the other sample was annealed after growth in 1 atm of O_2 for 1 h at 700°C (MBE-2-A).

PLD-1 samples were grown using either single crystalline STO (PLD-1) or sintered pressed ceramic STO (PLD-1-CER) as the source target. PLD-1 samples were grown on STO or LSAT substrates with an oxygen pressure of 50–100 mTorr. PLD-2 samples were grown using single crystalline STO as the source target, and an oxygen pressure of 100 mTorr. PLD-3 samples were grown using either single crystalline STO or sintered pressed STO (PLD-3-CER) as the source target and an oxygen pressure of 100 mTorr.

Film thicknesses were in the range 300–400 nm and were measured by RHEED during growth or by picosecond acoustics for films grown on LSAT substrates. [The (001) longitudinal speed of sound in STO (Ref. 21) is 7.9 nm/ps.] Each STO sample was coated with a ≈ 80 nm thick layer of Al that serves as the optical transducer for the TDTR measurement.

Our principal experimental results are summarized in Fig. 1 where we plot $\Lambda(T)$ for STO prepared by MBE [Fig. 1(a)] and PLD [Fig. 1(b)]. For both MBE and PLD, the best

epitaxial layers have $\Lambda(T)$ that closely approach bulk values, showing only a minor decrease in conductivity at the lowest temperatures we have measured, $T \approx 100$ K. Differences between MBE growth techniques and annealing conditions produce measurable but changes in thermal conductivity.

We can draw some important conclusions from these data. Extended defects and residual strain created by growth on a lattice mismatched substrate, e.g., LSAT with a lattice mismatch of 0.95%,¹¹ do not have a significant effect on thermal conductivity Λ at temperatures $T > 150$ K. The lack of sensitivity to residual strain is expected. The effect of strain on Λ can be estimated based on Leibfried-Schlomann equation which states that Λ should scale with the cube of the Debye temperature.^{22,23} Since the Grüneisen parameter of STO is ≈ 1.5 ,²¹ a volume strain of 1% produces a 1.5% change in the Debye temperature, and therefore a 4.5% change in thermal conductivity. Because the films are partially relaxed and the strain is biaxial, the residual strain of STO grown on LSAT is expected to produce a negligible change in Λ .

The effects of defects related to oxygen vacancies are revealed by comparing the “as-received” MBE-2 sample and the MBE-2-A sample that was deposited under identical conditions and then annealed in 1 atm of O_2 at 700°C for 1 h. The change in Λ in the temperature range $150 < T < 300$ K is 10%–17%. A decrease in Λ of up to $\sim 30\%$ was previously observed in highly oxygen deficient single crystalline STO.²⁴ We are not aware of any prior study that quantitatively relates oxygen vacancy concentrations to changes in thermal conductivity, and phonon scattering rates of point defects are difficult to estimate theoretically. We note, however, that a comparable change in thermal resistivity $\Delta(1/\Lambda) \approx 0.02$ m K W^{-1} of STO is produced by replacing 5% of the Sr sites with La (Ref. 24) and, in the well-studied SiGe alloy system, a comparable change in thermal resistivity of Si is produced by replacing 0.25% of the Si sites with Ge.²⁵

The thermal conductivity Λ of STO grown by PLD displays a surprising variety of behavior and a degree of sensitivity to experimental parameters that was unexpected. For example, films prepared at both UCB and UIUC show that growth from ceramic targets produces much lower Λ and, by inference, higher defect densities than films grown from single crystal STO targets. We can only speculate on the cause of this difference: the presence of grain boundaries or porosity is presumably altering the laser-target interactions and the composition of the laser plume.

In Fig. 2, we correlate changes in the out-of-plane lattice parameter of homoepitaxial PLD films with changes in Λ . Representative high resolution XRD results are shown in Fig. 2(a). (Different diffractometers were used at the different institutions but all data were acquired using energy-filtered and highly-collimated $\text{Cu } K\alpha_1$ radiation.) The STO (002) substrate peak appears at 46.47° and the film peak overlaps with the substrate peak for the MBE-1, PLD-2, and PLD-3-850 samples. (For PLD-3-850, we attribute the shoulder to the right of the substrate peak to originate from some portion of the mosaic within the substrate rather than the film. An extensive analysis of homoepitaxial STO films by Ohnishi *et al.*⁴ reported that diffraction by the films only appears to the left of the substrate peak.)

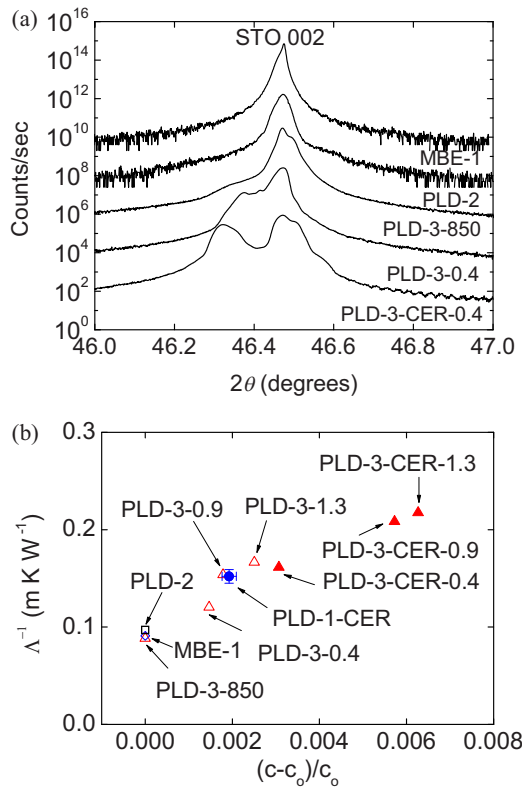


FIG. 2. (Color online) Comparison between changes in the out-of-plane lattice parameter of homoepitaxial PLD films grown on STO substrates with changes in thermal conductivity. (a) Representative high resolution XRD data of STO films grown on STO substrates. Curves are offset from each other vertically for clarity. PLD-3-850 and PLD-3-0.4 indicate STO films grown using a single crystalline target at 850 or 700 °C substrate temperature, respectively. PLD-3-CER-0.4 is a STO film grown using a sintered pressed ceramic target, substrate temperature of 700 °C, and deposition laser fluence of 0.4 J cm⁻². (b) Correlation between the thermal resistivity 1/Λ at room temperature of STO films grown by PLD and the change in the out-of-plane lattice constant of the film relative to the substrate. The error bars on the filled circle show the variations in thermal conductivity and lattice constant of as-received samples and samples annealed for 1, 4, and 16 h in 1 atm O₂.

For PLD films with nonoptimized deposition conditions, PLD-3-0.4 (single crystal target, substrate temperature of 700 °C, and deposition laser fluence of 0.4 J cm⁻²) and PLD-3-CER-0.4 (ceramic target, substrate temperature of 700 °C, and deposition laser fluence of 0.4 J cm⁻²), the film peak appears as a shoulder to the left of the substrate peak. Strain produced by defects in PLD films is known to be significantly larger than expected based on deviations of stoichiometry alone.²⁰ Freedman *et al.*²⁶ have suggested that point defects in samples grown by PLD involve complex clusters of defects with large defect volumes. The exact make-up of these defect clusters is not yet known. However, the additional thermal resistance created by these point defect clusters appears to scale with strain as shown in Fig. 2(b).

In conclusion, we have demonstrated the usefulness of thermal conductivity measurements by TDTR for characterizing the quality of epitaxial layers of oxides. The sensitivity of TDTR thermal conductivity measurements to point defect concentration depends on the details of phonon scattering rates but is on the order of 1%. TDTR is applicable to a wide variety of materials including electrically insulators that cannot be characterized by electrical transport measurements and heteroepitaxial layers where the lattice mismatch be-

tween film and substrate obscures shifts in lattice parameters created by point defects. We find that optimized growth conditions, specifically the use of single crystal laser targets and high substrate temperatures in PLD, lead to high thermal conductivities comparable to bulk.

This work was supported by U.S. Department of Energy, Office of Basic Energy Sciences, under Award Grant No. DE-FG02-07-ER-4645 and was carried out in part in the Frederick Seitz Materials Research Laboratory Central Facilities, University of Illinois, which are partially supported by the U.S. Department of Energy under Grant Nos. DE-FG02-07ER46453 and DE-FG02-07ER46471. The work at UCB (R.R.) was supported by the Division of Materials Sciences and Engineering of U.S. Department of Energy under Contract No. DE-AC02-05CH1123. J.R. acknowledges the Link Energy Fellowship and W.S. acknowledges support from the Dutch Organization for Scientific Research (NWO-Rubicon Grant). The work at UCSB (B.J. and S.S.) was supported as part of the Center for Energy Efficient Materials, an Energy Frontier Research Center funded by the U.S. Department of Energy, Office of Science, Office of Basic Energy Sciences under Award No. DE-SC0001009.

¹M. Imada, A. Fujimori, and Y. Tokura, *Rev. Mod. Phys.* **70**, 1039 (1998).

²J. M. D. Coey, M. Viret, and S. von Molnar, *Adv. Phys.* **48**, 167 (1999).

³M. Dawber, K. M. Rabe, and J. F. Scott, *Rev. Mod. Phys.* **77**, 1083 (2005).

⁴T. Ohnishi, M. Lippmaa, T. Yamamoto, S. Meguro, and H. Koinuma, *Appl. Phys. Lett.* **87**, 241919 (2005).

⁵N. Nakagawa, H. Y. Hwang, and D. A. Muller, *Nature Mater.* **5**, 204 (2006).

⁶M. Varela, S. D. Findlay, A. R. H. M. Lupini Christen, A. Y. Borisevich, N. Dellby, O. L. Krivanek, P. D. Nellist, M. P. Oxley, L. J. Allen, and S. J. Pennycook, *Phys. Rev. Lett.* **92**, 095502 (2004).

⁷M. Lippmaa, N. Nakagawa, M. Kawasaki, S. Ohashi, and H. Koinuma, *Appl. Phys. Lett.* **76**, 2439 (2000).

⁸S. V. Kalinin, B. J. Rodriguez, A. Y. Borisevich, A. P. Baddorf, N. Balke, H. J. Chang, L. Q. Chen, S. Choudhury, S. Jesse, P. Maksymovych, M. P. Nikiforov, and S. J. Pennycook, *Adv. Mater. (Weinheim, Ger.)* **22**, 314 (2010).

⁹P. Partyka, Y. Zhong, K. Nordlund, R. S. Averback, I. M. Robinson, and P. Ehrhart, *Phys. Rev. B* **64**, 235207 (2001).

¹⁰J. Son, P. Moetakef, B. Jalan, O. Bierwagen, N. J. Wright, R. Engel-Herbert, and S. Stemmer, *Nature Mater.* **9**, 482 (2010).

¹¹M. L. Scullin, C. Yu, M. Huijben, S. Mukerjee, J. Seidel, Q. Zhan, J. Moore, A. Majumdar, and R. Ramesh, *Appl. Phys. Lett.* **92**, 202113 (2008).

¹²G. A. Slack, *J. Phys. Chem. Solids* **34**, 321 (1973).

¹³D. G. Cahill and R. O. Pohl, *Annu. Rev. Phys. Chem.* **39**, 93 (1988).

¹⁴D. G. Cahill, *Rev. Sci. Instrum.* **75**, 5119 (2004).

¹⁵Y. K. Koh and D. G. Cahill, *Phys. Rev. B* **76**, 075207 (2007).

¹⁶K. Kang, Y. K. Koh, C. Chiritescu, X. Zheng, and D. G. Cahill, *Rev. Sci. Instrum.* **79**, 114901 (2008).

¹⁷See supplementary material at <http://dx.doi.org/10.1063/1.3579993> for a full description of the STO samples measured in this work.

¹⁸B. Jalan, P. Moetakef, and S. Stemmer, *Appl. Phys. Lett.* **95**, 032906 (2009).

¹⁹C. Yu, M. L. Scullin, M. Huijben, R. Ramesh, and A. Majumdar, *Appl. Phys. Lett.* **92**, 191911 (2008).

²⁰C. M. Brooks, L. F. Kourkoutis, T. Heeg, J. Schubert, D. A. Muller, and D. G. Schlom, *Appl. Phys. Lett.* **94**, 162905 (2009).

²¹A. G. Beattie and G. A. Samara, *J. Appl. Phys.* **42**, 2376 (1971).

²²M. Roufosse and P. G. Klemens, *Phys. Rev. B* **7**, 5379 (1973).

²³G. A. Slack, *Solid State Physics* (Academic, New York City, 1979), p. 35.

²⁴H. Muta, K. Kurosaki, and S. Yamanaka, *J. Alloys Compd.* **392**, 306 (2005).

²⁵D. G. Cahill, F. Watanabe, A. Rockett, and C. B. Vining, *Phys. Rev. B* **71**, 235202 (2005).

²⁶D. A. Freedman, D. Roundy, and T. A. Arias, *Phys. Rev. B* **80**, 064108 (2009).